



Fermi National Accelerator Laboratory

FERMILAB-Pub-90/149-A
July 25, 1990

Characteristic microwave background distortions from collapsing domain wall bubbles

GUENTER GOETZ

DIRK NÖTZOLD

*Astronomy and Astrophysics Center,
University of Chicago, Chicago IL 60637*

and

*NASA/Fermilab Astrophysics Center, Fermi
National Accelerator Laboratory, Batavia, IL 60510.*

ABSTRACT

We analyze the magnitude and angular pattern of distortions of the microwave background by collapsing spherical domain walls. We find a characteristic pattern of redshift distortions of red or blue spikes surrounded by blue discs. The width and height of a spike is related to the diameter and magnitude of the disc. A measurement of the relations between these quantities thus can serve as an unambiguous indicator for a collapsing spherical domain wall. From the redshift distortion in the blue discs we find an upper bound on the surface energy density of the walls $\sigma \lesssim 8 \text{ MeV}^3$.



A phase transition in the early universe that allows a scalar field to settle down in different vacuum expectation values in different regions of the universe would produce domain walls between these regions. However, it is well known that stable domain walls in the early universe would soon have dominated the energy density¹ and therefore domain walls were considered irrelevant in a cosmological context. The renewed interest in domain walls is due to a scenario of galaxy formation proposed by Hill, Schramm and Fry² in which these topological defects form after recombination and provide the seeds for the clustering of baryons. An important criterion for the viability of such a model of structure formation is whether the induced distortion of the microwave background is compatible with the observed isotropy.

In this paper we calculate the redshift distortion induced by collapsing spherical domain walls³. We find that they lead to a distinctive pattern in the angular temperature fluctuations of the microwave background.

A domain wall that comes within the cosmic horizon will collapse due to its surface tension. The collapse will proceed almost with the velocity of light until the radius of the bubble becomes comparable to the wall thickness and the wall decays into scalar bosons⁴. These bosons move outwards in a shell with a thickness comparable to that of the original wall. It is also possible that the bubble forms a black hole. Outside the collapsing bubble the gravitational field is equivalent to that of a point mass. Inside, however, because of the vanishing energy density, there is no gravitational field. A photon passing through the gravitational field of the bubble receives a shift in its energy (i.e. a red- or blueshift), mainly due to three effects⁵: (i) a shift in energy equal to the difference in the gravitational potential at the points where the photon enters and leaves the bubble. (ii) a change in the potential caused by the cosmic expansion. (iii) a time delay that photons traversing the gravitational potential suffer with respect to photons unaffected by the potential. In an expanding universe this last contribution always corresponds to a blue shift in the energy of the photon.

The net change in the energy of the photon depends on the gravitational field along the path of the photon. There are three qualitatively different trajectories (see Fig.1):

- (I) The photon passes outside the bubble and the redshift is determined by the Schwarzschild potential.
- (II) The photon traverses the bubble. Since the bubble wall collapses almost with the speed of light and the gravitational field vanishes inside the bubble the photon is redshifted only after leaving the bubble.

(IIIa) The photon crosses the expanding shell of bosons that are emitted in the final stage of the wall collapse. Since there is no gravitational field inside the shell the redshift distortion of the photons is given by the contribution they receive before entering the shell.

(IIIb) In case of black hole formation the photons always see a Schwarzschild field like in (I).

The redshift distortion⁶ in an expanding background $a^2\eta_{\mu\nu}$ ($\eta_{\mu\nu} = \text{diag}(1, -1, -1, -1)$) caused by a metric perturbation $a^2h_{\mu\nu}$ is given by

$$\frac{\delta E}{E} = -\frac{1}{2}h_{tt} + \frac{1}{2} \int dt \frac{\partial h_{\mu\nu}}{\partial t} a^4 \frac{dx_{(o)}^\mu}{dt} \frac{dx_{(o)}^\nu}{dt} \quad (1)$$

where the integral is to be evaluated along the unperturbed null geodesics $x_{(o)}^\mu(t)$. Here we consider a matter dominated flat background in conformal coordinates with a scale factor $a \propto t^2$. The metric perturbations at radius r around a point mass M in the adiabatic approximation, where all terms with \ddot{a}, \dot{a}^2 are neglected, are: $h_{tt} = h_{rr} = -2GM/(ar)$. Inserting these perturbations into (1) and evaluating the integral along the unperturbed photon path $r(t) = \sqrt{(t-t_*)^2 + r_*^2}$ where t_* is the time when the photon passes the bubble at a distance r_* , we find

$$\begin{aligned} \frac{\delta E}{E} = & 2GMH_c \left\{ \frac{r_*^4 - 10r_*^2t_*^2 + 4t_*^4}{4(r_*^2 + t_*^2)^{7/2}} \text{asinh} \left(\frac{t_*(t-t_*) - r_*^2}{r_*t} \right) \right. \\ & + \frac{1}{4(t_*^2 + r_*^2)^{3/2} \sqrt{(t-t_*)^2 + r_*^2}} \left[(7r_*^2 - 8t_*^2)t_*t^3 + (r_*^4 - 17r_*^2t_*^2 + 12t_*^4)t^2 + \right. \\ & \left. \left. + (3r_*^4 + r_*^2t_*^2 - 2t_*^4)t_*t - t_*^2(r_*^2 + t_*^2)^2 \right] \right\} \Bigg|_{t_i}^{t_f} \quad (2) \end{aligned}$$

Here we have normalized the time t , t_* and radius r_* with respect to t_c ($t_c = 1$), the time when the bubble is collapsed. $H_c = H_0(1+z_c)^{3/2}$ is the Hubble parameter at cosmic redshift z_c . Since the gravitational effects of the wall are limited by the horizon scale at time t_c we take for the range of integration in (2)

$$|t - t_c| \leq \left(\frac{1}{a} \frac{\partial a}{\partial t} \right)^{-1} \Rightarrow 2t_c/3 < t < 2t_c \quad (3)$$

where $a/\partial_t a$ is the cosmic expansion scale that also determines the region of validity of the adiabatic approximation. Similarly, t_* and r_* are restricted to the

range $2t_c/3 < t_* < 2t_c$, $r_* < t_c$. For the three different trajectories of the photon we therefore have:

$$\begin{aligned}
(I): \quad t_i &= 2/3t_c, \quad t_f = 2t_c \\
(II): \quad t_i &= \frac{t_c^2 - r_*^2 - t_*^2}{2(t_c - t_*)}, \quad t_f = 2t_c \\
(IIIa): \quad t_i &= 2/3t_c, \quad t_f = \frac{r_*^2 + t_*^2 - t_c^2}{2(t_* - t_c)} \\
(IIIb): \quad t_i &= 2/3t_c, \quad t_f = 2t_c
\end{aligned}$$

In (II) t_i is the time when the photon leaves the bubble which collapses with the speed of light and in (IIIa) t_f is the time when the photon crosses the boson shell which is assumed to expand with the speed of light. In the case that the above values for t_f exceed t_0 we take $t_f = t_0$.

When the bubble is at a coordinate distance r_c from us, a photon that passes the bubble center with impact parameters r_* and t_* will appear at an angle θ with respect to the bubble center: $r_* = r_c \sin \theta$, $t_* = t_0 - r_c \cos \theta$ where t_0 is the present epoch. The redshift distortion $\delta E/E$ is plotted as a function of θ in Fig. 2 at fixed cosmic redshift $1 + z_c = (t_0/t_c)^2$ and fixed $\xi \equiv (t_0 - t_c)/r_c$. Note that for $\xi > 1$ (< 1) we are located inside (outside) the future light cone of the collapse event and only photons with trajectories I,III (I,II) can be observed leading to the different qualitative behavior in Fig. 2 for $\xi > 1$ and $\xi < 1$. The small kinks in Fig. 2 for $\xi < 1$, where the curves attain their maximal blueshift, correspond to the boundary between region (I) and (II), $t_i(I) = t_i(II)$. They are a consequence of our approximation, eq. (3), and the assumption that the collapse proceeds with the speed of light. The angle θ_w at which the small kinks occur is approximately

$$\theta_w \approx \arccos \left[\frac{\xi + 3(\sqrt{1 + z_c} - 1)}{1 + 3(\sqrt{1 + z_c} - 1)} \right]. \quad (4)$$

θ_w is also a measure for the width of the spikes.

We also remark that $\delta E/E$ vanishes as θ goes to $\theta_H \equiv \arctan[1/(\sqrt{1 + z_c} - 1)]$, the angle subtended by the horizon at redshift z_c , since for an impact parameter $r_* > t_* \approx t_c$ photons are not affected by the gravitational field.

Photons from (I), that appear at angles $\theta > \theta_w$, are always blueshifted because the blueshift from the time delay always exceeds the redshift from the changing gravitational field⁷. It is also evident from Fig. 2 that photons from

(II) ($\xi < 1$) lead to red spikes at small angles. This is to be expected since the spikes occur when the photon leaves the bubble at small radii. During the time the photons traverse the bubble they do not experience a gravitational field and therefore, when leaving the bubble at small radii, they appear at the bottom of a deep Schwarzschild potential outside the bubble. Upon climbing out of this potential they lose energy, i.e. become redshifted. The Schwarzschild potential is deeper for smaller impact parameters $r_* \rightarrow 0$ and $t_* \rightarrow t_c$, therefore the height of the spikes increases for small angles θ_w . These features can also be seen from the formula (2) in the limit $r_* \rightarrow 0$, $t_* \rightarrow t_c$ when the second term which is inversely proportional to the distance of the photon from the bubble center, becomes large. Photons from (III) ($\xi > 1$) fall down the Schwarzschild potential until they cross the boson shell beyond which the gravitational potential is zero. Therefore, they get blueshifted. Since the gain in energy increases for small impact parameters the height of the spikes increases for small angles θ_w .

For larger values of ξ the height of the spikes decreases until they flatten out into disc-like structures. In this case the change of the gravitational field due to the cosmic expansion and the time delay give the main contributions.

To summarize, we have found that collapsing spherical domain walls give rise to very distinctive redshift patterns of red or blue spikes surrounded by a region where the blueshift falls off towards larger angles. The spikes cover a fraction θ_w of a blue disc that gradually varies over an angle θ_H . The height of the spikes is approximately given by

$$\left. \frac{\delta E}{E} \right|_{\text{spike}} \approx 2GMH_c \frac{1}{2(\sqrt{1+z_c}-1)} \frac{\xi}{\xi-1} \quad (5)$$

whereas the blue disc has an intensity of $\delta E/E \approx 2GMH_c$. The amplitude of the angular redshift pattern increases with decreasing cosmic redshift as $2GMH_c \propto (1+z_c)^{-3/2}$, since the mass of a bubble that begins to collapse at about $t_c/2$ is given by $M = 4\pi\sigma H_c^{-2}/16$ where σ is the surface energy density of the domain wall. Therefore, the overall amplitude is larger for domain bubbles collapsing at lower redshifts. Also, at lower cosmic redshift the spike becomes more pronounced since the magnitude of the spike increases with respect to the surrounding blue disc.

We point out that a measurement of the width and the magnitude of a spike and a blue disc would allow one to decide whether the signal is caused by collapsing spherical domain walls. The angular extent of the blue disc θ_H would determine z_c and the width of the spike θ_w would give ξ . Then, if the signal is

due to a collapsing bubble the contrast of the spike relative to the background must be:

$$\frac{\delta E}{E}|_{\text{spike}} / \frac{\delta E}{E}|_{\text{backgr.}} \approx \frac{\xi}{2(\sqrt{1+z_c}-1)(\xi-1)} \quad (6)$$

That is, the verification of the relations between these quantities would be an *unambiguous indicator for collapsing domain walls*. In addition, the absolute magnitude of the spike would determine the surface energy density of the walls.

Although the existence of spikes suggests the possibility of a strong bound on the surface energy density σ , we now argue that the only reliable bound comes from the blue discs created by bubbles collapsing at low cosmic redshifts: $\delta E/E \approx \pi G \sigma H_0^{-1}/2$. To create spikes with a larger redshift distortion than the disc $\delta E/E|_{\text{spike}} \gtrsim \pi G \sigma H_0^{-1}/2$ the collapsing bubbles have to be close to our past lightcone: $|1-\xi| \lesssim [2(\sqrt{1+z_c}-1)(1+z_c)^{3/2}]^{-1}$. The number density of collapsing bubbles per comoving volume is about⁸ $dN/(dt dV) \approx t^{-4}$. Therefore the total number of bubbles collapsing in a redshift interval dz_c around z_c that give rise to spikes higher than the blue discs from bubbles collapsing at low redshift is bounded by

$$\frac{dN}{dz_c} \lesssim \frac{2\pi}{(1+z_c)^{3/2}} \quad (7)$$

which gives $N \lesssim 4$ for the total number at all redshifts. One sees that spikes exceeding the blue discs from low redshifts are quite rare.

To obtain a conservative bound on σ we consequently take the redshift distortion in the blue discs created by bubbles collapsed at low cosmic redshift $\delta T/T \equiv \delta E/E \approx \pi G \sigma H_0^{-1}/2$ (see Fig. 2). This has to be compared with the upper bound on the temperature fluctuations⁹ $\delta T/T \lesssim 4 \times 10^{-5}$ on angular scales $\theta \lesssim 10^\circ$. So, we arrive at the upper bound for $\sigma \approx 2.0 h 10^{-4} \text{ GeV}^3 (\delta T/T) \lesssim 8 h \text{ MeV}^3$ with $H_0 = 100h \text{ km sec}^{-1} \text{ Mpc}^{-1}$ and $0.4 \lesssim h \lesssim 1$.

Finally, we consider the redshift distortion in the microwave background that would be induced by spherical domain walls collapsing into black holes. A condition for black hole formation from domain wall bubbles was discussed by Widrow⁴. For $\xi < 1$ the photons fly outside the future lightcone of the collapse event and are therefore not influenced by the black hole. The redshift distortion for $\xi < 1$ is thus the same as in the case discussed above (see Fig. 2). For $\xi > 1$ the photons initially move in the Schwarzschild potential of the collapsing domain wall and after the collapse in the potential of the black hole. The photons along these

trajectories receive a net blueshift as a result of the time delay and the change in the gravitational field which is due to the cosmic expansion⁷. We have to choose the trajectories (IIIb) to evaluate the redshift distortion (2). The result is plotted in Fig. 3. In the limit of small impact parameter r_* (2) is well approximated by

$$\frac{\delta E}{E} = \pi G \sigma H_0^{-1} \frac{-\ln[(\sqrt{1+z_c}-1)\sin\theta/\xi] - 19/16}{(1+z_c)^{3/2} [(1-1/\xi)\sqrt{1+z_c} + 1/\xi]^3} \quad (8)$$

which shows a logarithmic growth for $\theta \rightarrow 0$. However, there is a minimal value of θ corresponding to the Schwarzschild radius \mathcal{R} of the black hole where $\delta E/E$ reaches a maximum. Note that for small \mathcal{R} the maximal redshift distortion decreases as $-\mathcal{R} \ln \mathcal{R}$. As shown in Fig. 3 domain wall bubbles collapsing to a black hole produce blue spikes on small angular scales, besides the wider red spikes already discussed above. Although good constraints on the isotropy of the microwave background on small scales exist¹⁰ it is not reasonable to use these constraints to derive an upper bound on σ , because the probability to find a collapse event at low redshifts on these angular scales is vanishingly small.

We found that the most frequent microwave background distortions occur on large angles in the form of blue discs. This is the angular region ($\theta > 7^\circ$) currently measured by the COBE-satellite. It therefore could detect signals predicted in this paper for domain walls with surface energy density of the order of MeV^3 . Such values for σ are proposed in the late time phase transition scenario of Hill, Schramm, Fry².

Acknowledgements

We thank David Schramm for encouragement. This work was supported by NSF AST88-22595 and NASA-NAGW-1321 at Chicago, by NASA-NAGW-1340 at Fermilab and by a Feodor-Lynen-fellowship of the Alexander-von-Humboldt foundation (G. G.).

REFERENCES

1. Ya. Zeldovich, I.Yu. Kobzarev and L.B. Okun, *Zh. Eksp. Teor. Fiz.* 67 (1974) 3 [*Sov. Phys. JETP* 40 (1975) 1]
2. Ch.T. Hill, D.N. Schramm and J. Fry, *Com. Nucl. Part. Phys.* 19 (1989) 25; Ch.T. Hill, D.N. Schramm and L.M. Widrow, Fermilab-Pub-89/166-T, preprint, 1989.
3. This is part of a larger project where we studied the redshift distortion of planar and spherical walls in dependence of the wall thickness, surface density, scalar field potential and cosmic redshift, Ref. 7.
4. L.M. Widrow, *Phys. Rev. D* 40 (1989) 1002.
5. M.J. Rees and D.W. Sciama, *Nature* 217 (1968) 511
6. R.K. Sachs and A.M. Wolfe, *Astrophys. J.* 147 (1967) 73
7. G. Goetz and D. Nötzold, to be published.
8. W.H. Press, B.S. Ryden and D.N. Spergel, *Astrophys. J.* 347 (1989) 590.
9. R.D. Davies et al., *Nature* 326 (1987) 462.
10. C.J. Hogan and R.B. Partridge, *Astrophys. J.* 341 (1989) L29.

FIGURE CAPTIONS

1. Space-time diagram for different photon trajectories.
2. Redshift distortion as a function of angle θ for different values of ξ at cosmic redshift: (a) $z_c = 1$, (b) $z_c = 10$.
3. Redshift distortion by a black hole for $\xi > 1$.

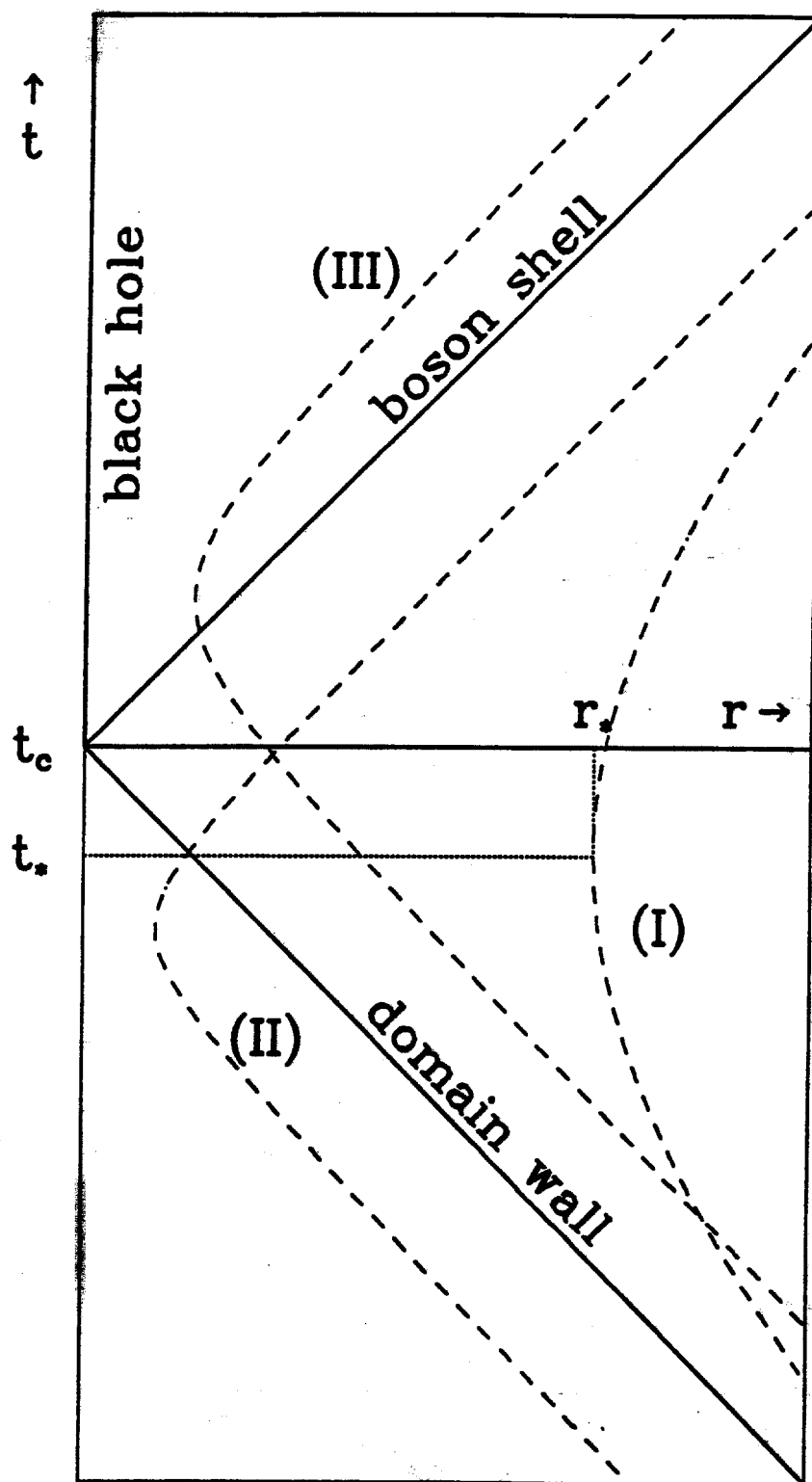


Fig. 1.

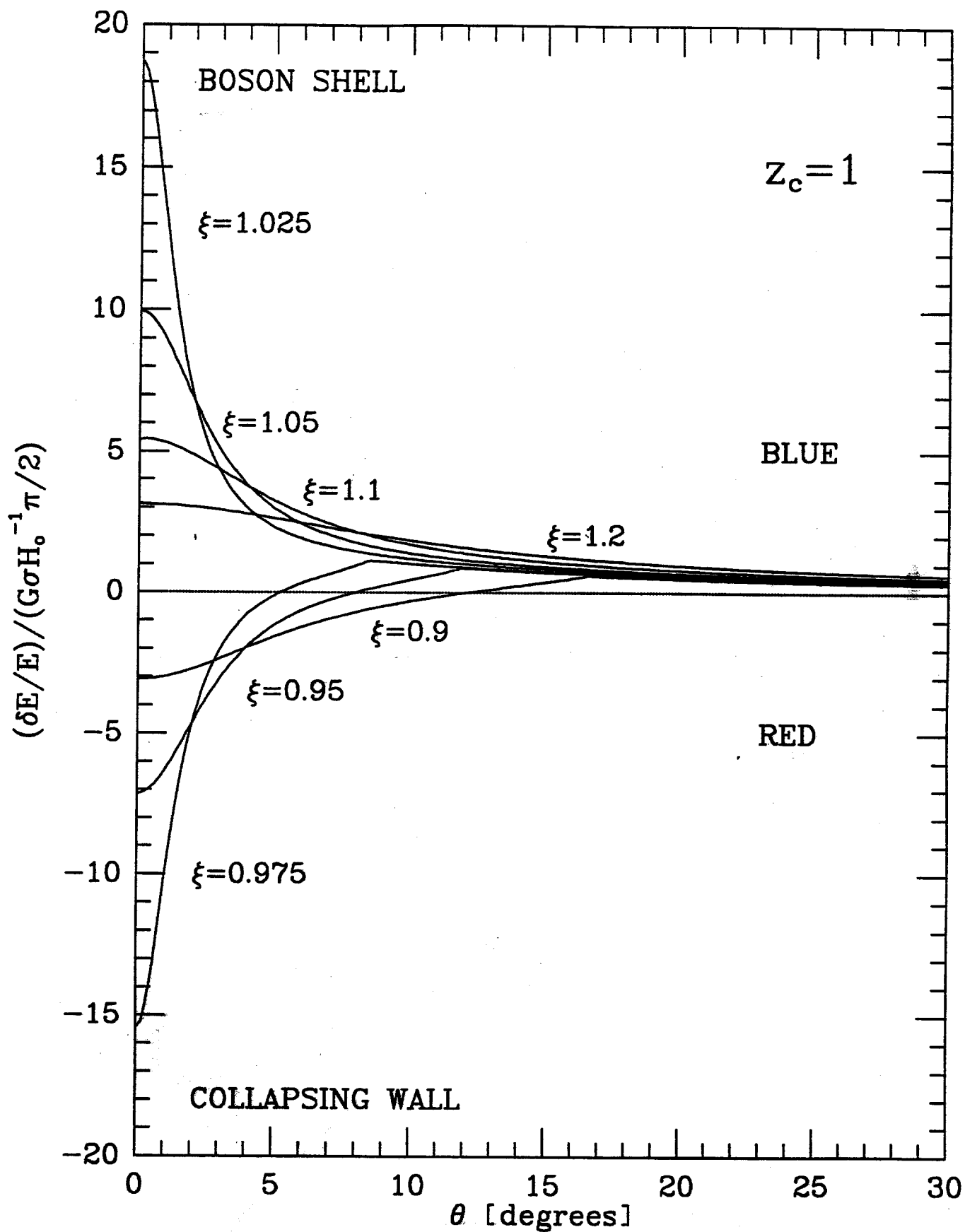


Fig. 2a

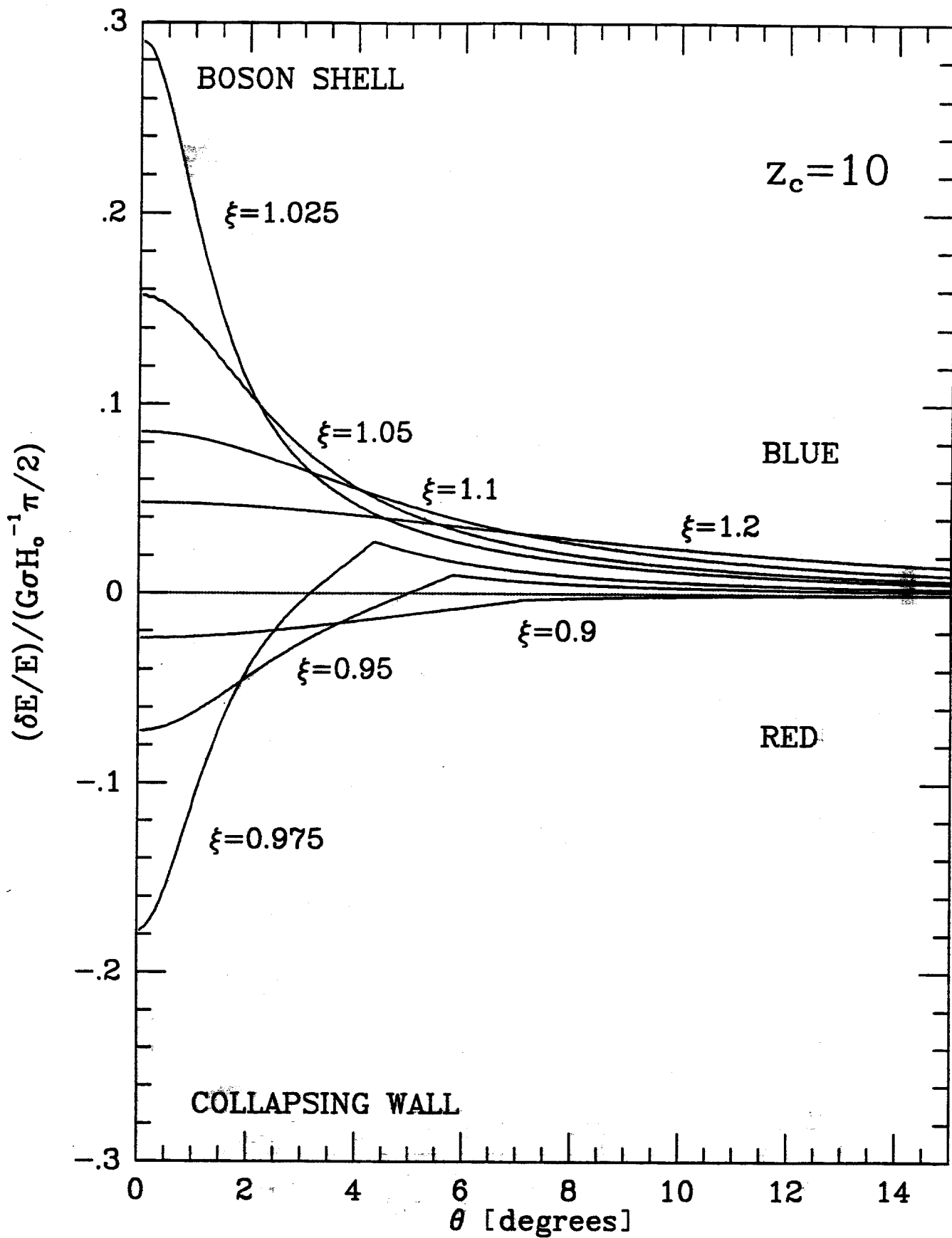


Fig. 26

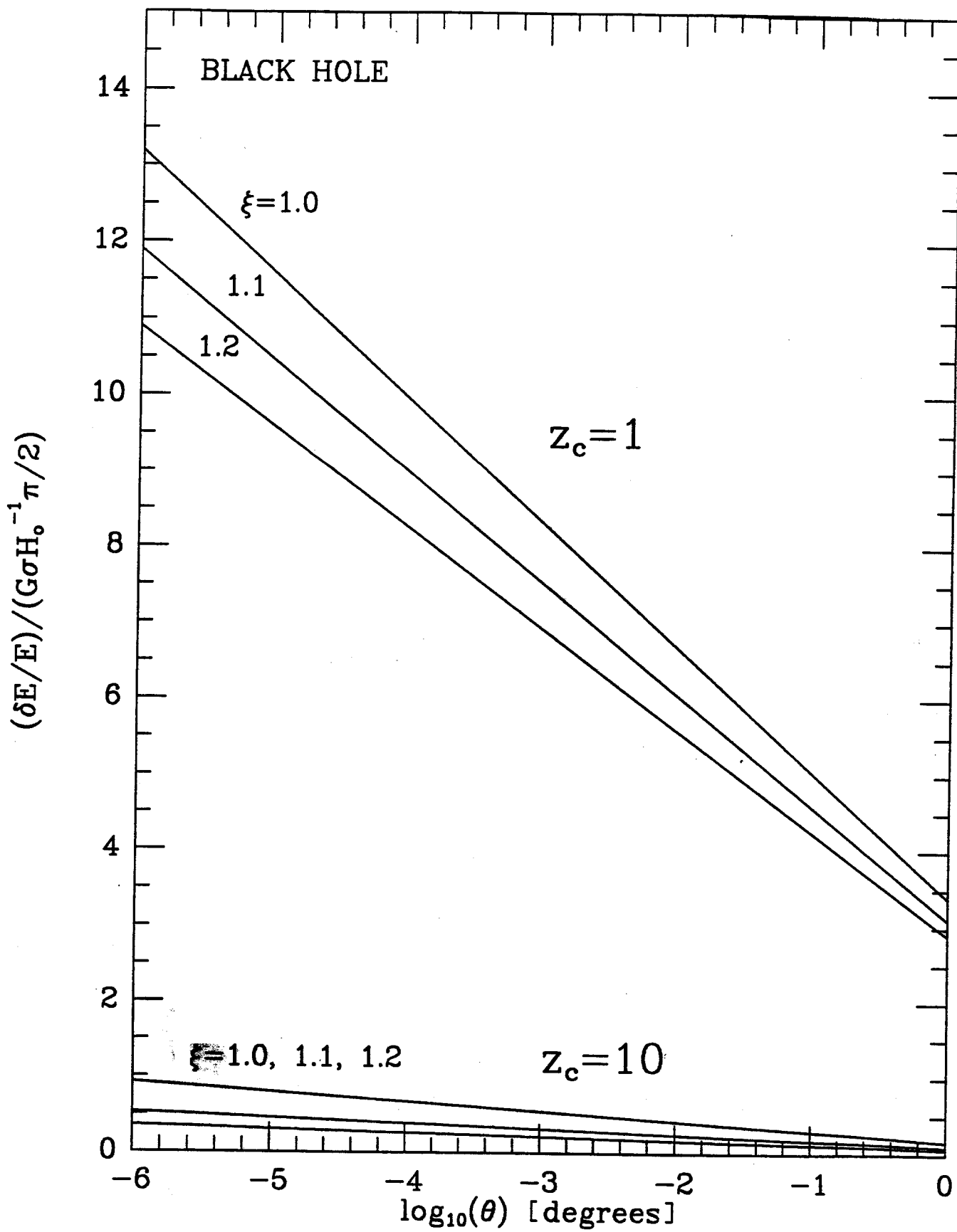


Fig. 3